

# The influence of defects on magnetic properties of fcc-Pu

A. O. Shorikov, M. A. Korotin, V. I. Anisimov

*Institute of Metal Physics, Ural Division of Russian Academy of Sciences, 18, S. Kovalevskaya str., 620041 Ekaterinburg GSP-170, Russia*

V. V. Dremov, Ph. A. Sapozhnikov

*Russian Federal Nuclear Center - Institute of Technical Physics, 13, Vasiliev str., Snezhinsk, 456770 Chelyabinsk region, Russia*

---

## Abstract

The influence of vacancies and interstitial atoms on magnetism in Pu has been considered in frames of the Density Functional Theory (DFT). The relaxation of crystal structure arising due to different types of defects was calculated using the molecular dynamic method with modified embedded atom model (MEAM). The LDA+U+SO (Local Density Approximation with explicit inclusion of Coulomb and spin-orbital interactions) method in matrix invariant form was applied to describe correlation effects in Pu with these types of defects. The calculations show that both vacancies and interstitials give rise to local moments in  $f$ -shell of Pu in good agreement with experimental data for annealed Pu. Magnetism appears due to destroying of delicate balance between spin-orbital and exchange interactions.

*Keywords:* actinide alloys and compounds, electronic band structure, computer simulations

*PACS:* 74.25.Jb, 71.27.+a, 71.45.Gm

---

## 1. Introduction

Band structure calculations of  $\delta$ -Pu predict the static magnetic order of  $f$ -electrons with the values of full magnetic moment  $0.25\text{--}5 \mu_B$  with substantial impact of spin moment [1, 2, 3, 4]. These results contradict to experimental measurements of magnetic properties of non-aged Pu without impurities. These data indicate the absence of any ordered or disordered, static or dynamic magnetic moments in Pu at low temperatures [5, 6].

Recent development of calculation methods allows to describe correctly the ground state of pure Pu in  $\delta$ - and model  $\alpha$ -phase [8, 7]. It has been shown in Ref. [7] that the delicate balance between spin-orbit (SO) and exchange interactions determines the nonmagnetic ground state in pure Pu. These interactions have the magnitude close to each other in actinides and its compounds and the

---

*Email address:* v.v.dremov@vniitf.ru (V. V. Dremov)

balance could be easily broken by crystal field of legands. Also, P. Söderlind [9] confirs the important role of SO and orbital polarization in formation of non-magnetic ground state of plutonium in frames of model DFT calculation. Impurities like Al and Ga that are used to stabilize the fcc-phase of Pu act in the same way. Several groups report the presence of ordered magnetic moment in aged Pu-Al and Pu-Ga alloys [10, 11, 12]. The magnitude of moments is small,  $\leq 10^{-3} \mu_B$  (Ref. [10]) –  $0.15 \mu_B$  (Ref. [11, 12]), and these moments could arise due to distortion of crystal structure near interstitial Pu atoms and vacancies.

Substantial drawback of the Local (Spin) Density Approximation (L(S)DA) is the underestimation of orbital moment [13, 14]. This feature leads to fail of the DFT in description of  $4f$ - and  $5f$ -metals, since orbital moment in them can overcome spin one. Taking into account the Coulomb repulsion  $U$  and SO interactions in full matrix rotation invariant form in the LDA+U+SO method could improve the results. Achievement of this method is that one shouldn't set the exact magnetic order at the start of iterations. Both magnitude and direction of magnetic moment are calculated for each atom. Magnetic order and direction of "easy axis" are the result of self-consistent interaction procedure.

In the LDA+U method[15] the energy functional  $E_{LDA+U}$  depends, in addition to the charge density  $\rho(\mathbf{r})$ , on the occupation matrix  $n_{mm'}^{ss'}$  for particular orbital for which correlation effects are taken into account (in our case it is  $5f$  plutonium orbitals). The LDA+U method in general nondiagonal in spin variables form was defined in Ref. [16]

$$E_{LDA+U}[\rho(\mathbf{r}), \{n\}] = E_{LDA}[\rho(\mathbf{r})] + E_U[\{n\}] - E_{dc}[\{n\}] \quad (1)$$

where  $\rho(\mathbf{r})$  is the charge density,  $E_{LDA}[\rho(\mathbf{r})]$  is the standard LDA functional. The occupation matrix is defined as

$$n_{mm'}^{ss'} = -\frac{1}{\pi} \int^{E_F} \text{Im} G_{mm'}^{ss'}(E) dE \quad (2)$$

where  $G_{mm'}^{ss'}(E) = \langle ms | (E - \hat{H}_{LDA+U})^{-1} | m' s' \rangle$  are the elements of the Green function matrix in local orbital basis set ( $m$  – magnetic quantum number, and  $s$  – spin index for correlated orbital). In the present work this basis set was formed of LMT-orbitals from the tight binding LMTO method based on the atomic sphere approximation (TB-LMTO-ASA). [17] In Eq. (1) Coulomb interaction energy  $E_U[\{n\}]$  term is a function of occupation matrix  $n_{mm'}^{ss'}$

$$E_U[\{n\}] = \frac{1}{2} \sum_{\{m\}, \{s\}} \{ \langle m, m'' | V_{ee} | m', m''' \rangle n_{mm'}^{ss'} n_{m''m'''}^{s's'''} - \langle m, m'' | V_{ee} | m''', m' \rangle n_{mm'}^{ss'} n_{m''m'''}^{s's'''} \} \quad (3)$$

where  $V_{ee}$  is the screened Coulomb interaction between the correlated electrons. Finally, the last term in Eq. (1) correcting for double counting is a function of the total number of electrons in the spirit of LDA which is a functional of total charge density

$$E_{dc}[\{n\}] = \frac{1}{2} U N(N-1) - \frac{1}{4} J_H N(N-2) \quad (4)$$

where  $N = \text{Tr}(n_{mm'}^{ss'})$  is a total number of electrons in the particular shell.  $U$  and  $J_H$  are screened Coulomb and Hund exchange parameters which could be

determined in the constrain LDA calculations. [19, 18] The screened Coulomb interaction matrix elements  $\langle m, m'' | V_{ee} | m', m''' \rangle$  could be expressed via parameters  $U$  and  $J_H$  (see Ref. [15]).

The functional Eq. (1) defines the effective single-particle Hamiltonian with an orbital dependent potential added to the usual LDA potential

$$\hat{H}_{LDA+U} = \hat{H}_{LDA} + \sum_{ms, m's'} |ms\rangle V_{mm'}^{ss'} \langle m's'|, \quad (5)$$

$$\begin{aligned} V_{mm'}^{ss'} &= \delta_{ss'} \sum_{m'', m'''} \{ \langle m, m'' | V_{ee} | m', m''' \rangle n_{m''m'''}^{-s, -s} + \\ &(\langle m, m'' | V_{ee} | m', m''' \rangle - \langle m, m'' | V_{ee} | m''', m' \rangle) n_{m''m'''}^{ss} \} - \\ &(1 - \delta_{ss'}) \sum_{m'', m'''} \langle m, m'' | V_{ee} | m''', m' \rangle n_{m''m'''}^{s's} \\ &- U(N - \frac{1}{2}) + \frac{1}{2} J_H(N - 1). \end{aligned} \quad (6)$$

In this paper we used method LDA+U+SO which comprises non-diagonal in spin variables LDA+U Hamiltonian Eq. (6) with spin-orbit (SO) coupling term

$$\hat{H}_{LDA+U+SO} = \hat{H}_{LDA+U} + \hat{H}_{SO}, \quad (7)$$

$$\hat{H}_{SO} = \lambda \cdot \mathbf{L} \cdot \mathbf{S}$$

where  $\lambda$  is a parameter of spin-orbit coupling. In  $LS$  basis SO coupling matrix has diagonal  $(H_{SO})_{m',m}^{s,s}$  as well as off-diagonal in spin variables  $(H_{SO})_{m',m}^{\uparrow,\downarrow}$  and  $(H_{SO})_{m',m}^{\downarrow,\uparrow}$  non-zero matrix elements (in complex spherical harmonics)[? ]

$$\begin{aligned} (H_{SO})_{m',m}^{\uparrow,\downarrow} &= \frac{\lambda}{2} \sqrt{(l+m)(l-m+1)} (\delta_{m',m-1}), \\ (H_{SO})_{m',m}^{\downarrow,\uparrow} &= \frac{\lambda}{2} \sqrt{(l+m)(l-m+1)} (\delta_{m'-1,m}), \\ (H_{SO})_{m',m}^{s,s} &= \lambda m s \delta_{m',m} \end{aligned} \quad (8)$$

where  $lm$  - orbital quantum numbers, spin index  $s = +1/2, -1/2$ . The peculiarities of LDA+U+SO method and its implemenataion to the problem of pure Pu an several plutonium compounds were described in detales in Ref. [7].

In the present work four different fcc-Pu supercells were investigated. Namely: one interstitial (IS) Pu atom in 32-atoms supercell, vacancy in 8-atoms supercell, and two 32-atoms supercells with both IS and vacancy at minimal and large distances. Due to the presence of defects the perfect fcc structure was to be distorted and therefore the relaxation of crystal structure for all supercells under investigation should to be taken into account. Since LMTO method doesn't make possible to perform structure relaxation correctly we used Classical Molecular Dynamics (CMD) with the Modified Embedded Atom Model (MEAM) by Baskes [20, 21, 22] as interatomic potential. The MEAM is the many-body potential, i.e. interaction between a pair of atoms depends on the local structure (on positions of their common neighbors). The parametrization of the MEAM for pure plutonium and plutonium-gallium alloys was given in Ref. [20] and presently the potential is widely used in CMD simulations of plutonium properties and processes in Pu caused by self-irradiation (Refs. [20, 21, 22, 23, 24]).

Table 1: Magnetic properties calculated for 32-atoms supercell and interstitial (IS) Pu atom. First column – the labels of nonequivalent Pu atoms. Second column – distance between IS and Pu ion (Å). Next four columns: number of equivalent Pu atoms in subclasses ( $n_{atoms}$ ), calculated values for spin ( $S$ ), orbital ( $L$ ), and total ( $J$ ) moments. Last four columns contain partial contributions of  $f^6$  configurations and  $jj$ -type of coupling for  $5f$  shell of Pu ion, effective magnetic moment (see text for explanations) and total number of  $f$ -electrons.

	D, Å	$n_{atoms}$	$S$	$L$	$J$	$f^6, \%$	$jj, \%$	$\mu_{eff}$	$n_f$
IS		1	.028	.057	.03	98.9	99.2	.146	6.06
Pu1	2.79	4	.260	.341	.08	96.7	91.7	.234	5.69
		2	.065	.059	.01	99.8	97.8	.061	
Pu2	4.03	4	.216	.310	.09	96.3	93.2	.256	5.79
		4	.197	.277	.08	96.8	93.8	.238	
Pu3	5.22	4	.506	.633	.13	94.9	83.5	.271	5.77
		8	.380	.472	.09	96.3	87.7	.236	
Pu4	6.96	4	.750	1.111	.36	85.6	75.7	.456	5.73
		2	.471	.574	.10	95.9	84.6	.246	

Adding of IS or vacancy into initial supercell made Pu atoms inequivalent. That is why the different types of atoms in Tables below have additional numbers (e.g., Pu1 etc). The relaxation of crystal structure lowers the symmetry again, and the new Pu classes have been divided on sub-classes (see Tab. 1). All calculations of the electronic structure and magnetic properties were made using the Tight-Binding Linear Muffin-Tin Orbitals method with Atomic Sphere Approximation (TB-LMTO-ASA computation scheme). In the LDA+U calculation scheme the values of direct Coulomb ( $U$ ) and Hund’s exchange ( $J_H$ ) parameters should be determined as the first step of calculation procedure. It can be done in *ab initio* way via the constrained LDA calculations [18, 19]. In our calculations the Hund exchange parameter  $J_H$  was found to be  $J_H = 0.48$  eV. The value of Coulomb parameter  $U$  was set to 2.5 eV since this value provides the correct equilibrium volume of  $\delta$ -Pu (see Ref. [7] for the details).

## 2. Interstitial Plutonium atom in 32-atoms supercell

At first 32-atoms supercell of fcc-Pu with one additional Pu atom has been considered. The supercell has three coordination spheres around defect that is sufficient to describe relaxation of position of neighbor atoms. Classical molecular dynamic method was applied of describe distortion of crystal structure. New positions of Pu atoms in supercell were used in further calculation of electronic structure. Adding of one additional Pu atom lowers the symmetry of the cell. Four new inequivalent classes of plutonium belonging to four different coordination spheres around IS arouse. Moreover Pu atoms within each new class become inequivalent due to different local neighborhood. To take in to account this lowering of symmetry no symmetrisation was applied in our electronic structure calculation. Since no additional symmetry conditions was imposed on electronic subsystem magnitude of local moments on Pu sites and their directions can be arbitrary and correspond to the minimum of total energy.

The LDA+U+SO calculations for metallic Pu in  $\delta$  phase gave a nonmagnetic ground state with zero values of spin  $S$ , orbital  $L$ , and total  $J$  moments [8, 7]. Our calculation made for 32-atoms supercell with one IS shows that small local

magnetic moments develop on Pu sites. The magnitude of local moment depends on the distance between center of distortion (IS) and corresponding Pu site. We argue that this appears because of the break of balance between SO and exchange interactions due to the relaxation of crystal structure. The results are presented in Tab. 1. The partial contributions of  $f^6$  configuration and  $jj$ -type of coupling to the final state could be calculated in the following way. Total moment value is the same in both coupling schemes ( $jj$  or  $LS$ ):  $J = 0$  for  $f^6$  and  $J = 5/2$  for  $f^5$ . If there is a mixed state  $(1-x) \cdot f^6 + x \cdot f^5$  then  $x$  can be defined as  $x = J/2.5$ . Spin  $S$  and orbital  $L$  moment values for  $f^6$  configuration are equal to zero in  $jj$  coupling scheme and  $S = 3$ ,  $L = 3$  in  $LS$  coupling scheme. For  $f^5$  configuration they are  $S = 5/14 \approx 0.36$ ,  $L = 20/7 \approx 2.86$  in  $jj$  coupling scheme and  $S = 5/2$ ,  $L = 5$  in  $LS$  coupling scheme. One can define a mixed coupling scheme with a contribution of  $jj$  coupling equal to  $y$  and of  $LS$  coupling to  $(1-y)$ , correspondingly. In final state the calculated values of orbital and spin moments will be:

$$L = x \cdot (2.86 \cdot y + 5 \cdot (1-y)) + (1-x) \cdot (0 \cdot y + 3 \cdot (1-y)), \quad (9)$$

$$S = x \cdot (0.36 \cdot y + 2.5 \cdot (1-y)) + (1-x) \cdot (0 \cdot y + 3 \cdot (1-y)). \quad (10)$$

These formulas allow to determine the value of coefficient  $y$ . An effective paramagnetic moment obtained from susceptibility measurements using Curie-Weiss law can be calculated as

$$\mu_{eff} = g \cdot \sqrt{J \cdot (J+1)} \cdot \mu_B. \quad (11)$$

The problem is to define Lande  $g$ -factor which can be calculated for pure  $f^5$  and  $f^6$  configurations in  $LS$  or  $jj$  coupling schemes. As for  $f^6$  configuration total moment  $J = 0$ , one needs to calculate  $g$ -factor for  $f^5$  configuration only. For ground state of  $f^5$  configuration in  $jj$  coupling scheme Lande factor is  $g_{jj} = 6/7 \approx 0.86$ . In  $LS$  coupling scheme its value is  $g_{LS} = 2/7 \approx 0.29$ . As the latter value is nearly three times larger than the former,  $g_{jj}$  and  $g_{LS}$  can give only upper and lower limits of  $g$ -factor for the case of intermediate coupling. We could calculate weighted value of effective moment using relative weights of  $LS$ - and  $jj$ -couplings obtained from Eqs. 9, 10, 11.

The magnetic order of Pu ions is set arbitrary at the beginning of iteration process. Final directions of local moments are calculated in accordance with minimum of total energy at the end of self-consistence loop. Since the long range order is set up in used calculation method, some ferrimagnetic order arouse as an artifact. This order resembles the antiferromagnetic (AFM) one of A-type. In Fig. 1 resulting directions of total moment are shown with red and green colors. Pu atoms positioned in the first coordination sphere to IS as well as IS itself have the smallest magnetic moments. They don't differ significantly from pure  $\delta$ -Pu that is nonmagnetic. The values of local moments grow up with increasing distance between IS and corresponding site. The largest total moment developed for Pu4 ion positioned in the center of supercell (large red sphere in Fig. 1). This ion has the largest distance to IS. The average value of the effective moment in the case of IS Pu atom in 32-atoms supercell is  $\mu_{eff} \sim 0.26 \mu_B$ . Numbers of  $f$ -electrons (see Tab. 1 last column) differ from those calculated for not distorted fcc-Pu (which has 5.74  $f$ -electrons) but not significantly except the case of interstitial atom. The later has the largest occupation number in all

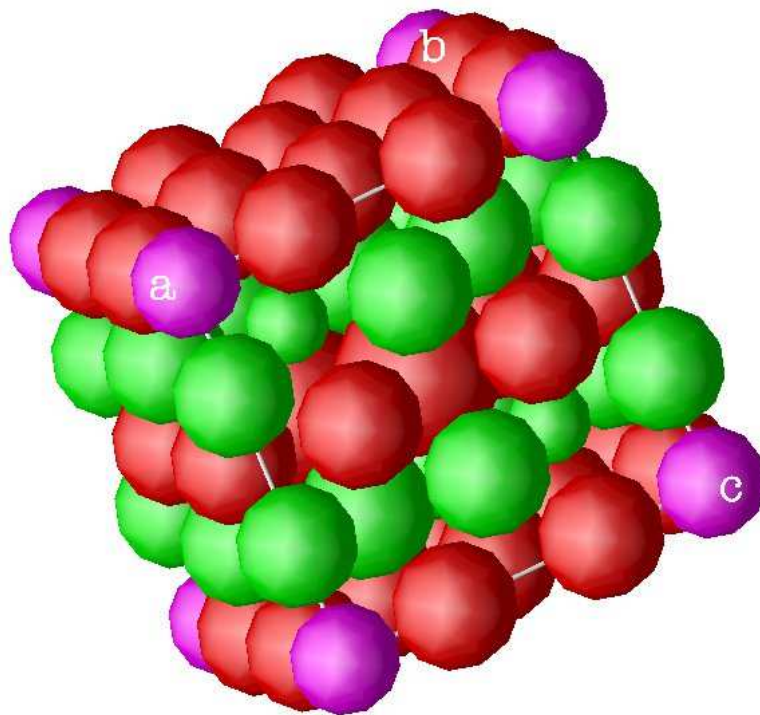


Figure 1: (Color online). Non-collinear order obtained for 32-atoms supercell with IS. Purple spheres denote IS. Green and red spheres are Pu atoms with opposite directed total moments. The radii of spheres are proportional to the magnitude of correspondent magnetic moments.

Table 2: Magnetic properties of Pu ions calculated for 8-atoms supercell with one vacancy. Second column – distance between vacancy and Pu ion (Å). See also the caption of Tab. 1.

	D, Å	$n_{atoms}$	$S$	$L$	$J$	$f^6, \%$	$jj, \%$	$\mu_{eff}$	$n_f$
Pu1	3.27	2	.651	.817	.166	93.4	78.7	.298	5.71
		2	.518	.656	.138	94.5	83.1	.283	
		2	.515	.652	.137	94.5	83.3	.283	
Pu2	4.63	1	.356	.449	.094	96.3	88.5	.243	5.70

considered structures (see tables below). The large number of  $f$ -electrons (close to 6) obtained in the present calculation disagrees with previous experimental and theoretical estimations that give 5.1-5.2 electrons[25]. Such difference between theoretical results originates from dissimilar band structure calculation methods. Since TB-LMTO-ASA scheme use artificially large overlapping atomic spheres these numbers should be considered only to compare different classes of plutonium atoms with each other. We have verified our results and run several calculations with different radii of Pu atoms filling of empty space in the primitive cell with empty spheres (pseudo-atom without core states). Distorted supercell always becomes magnetic with the same order. The magnitude of local magnetic moments depends slightly on atomic radius. It rises up with increasing of the later. For the sake of simplicity we have chosen the same radii 3.41 a.u. for all Pu atoms to be able to compare their magnetic moments. Artificial overlapping of atomic spheres in all considered supercells never overcomes 13% which is critical TB-LMTO-ASA value.

### 3. Vacancy in 8-atoms supercell

Another type of defects appearing in fresh Pu during first several years [26] is vacancy. Small supercell consisting of 8 Pu atoms was considered. One Pu atom was removed from its position in the supercell and after relaxation of crystal structure this empty space was artificially filled with empty sphere. Unfortunately, 8-atoms supercell is not sufficient to describe correctly the relaxation of crystal structure within the MEAM. Shifts of Pu atoms were obtained to be negligible. Nevertheless removing of one atom from the supercell lowers the symmetry of crystal, since the local neighborhood of plutonium atoms becomes different. Note, that this turns out enough to give rise to the local moments on Pu sites. Opposite to IS action, the vacancy affects much larger on Pu1 that form the first coordination sphere of it (Tab. 2). Magnetic moments of Pu2 atoms that belong to the 2-nd coordination sphere are smaller.

The average value of the effective magnetic moment in the supercell with vacancy is  $\sim 0.28 \mu_B$ . In contrast to the case of IS in 32-atoms supercell, the resulted magnetic order is the analogue of C-type AFM (see Fig. 2).

These results prove that both types of defects call local magnetic moment on Pu atoms due to distortion of fcc structure or even lowering of symmetry. Different types of defects affect magnetism in Pu in different ways: IS calls the largest magnetic moment on an atom at large distance whereas vacancy affects mostly its nearest neighbors. Different types of defects result also in different types of AFM order. Simultaneous effect of IS and vacancy could also give rise to the local moments and lead to more complicated pattern of Pu ions magnetic order.

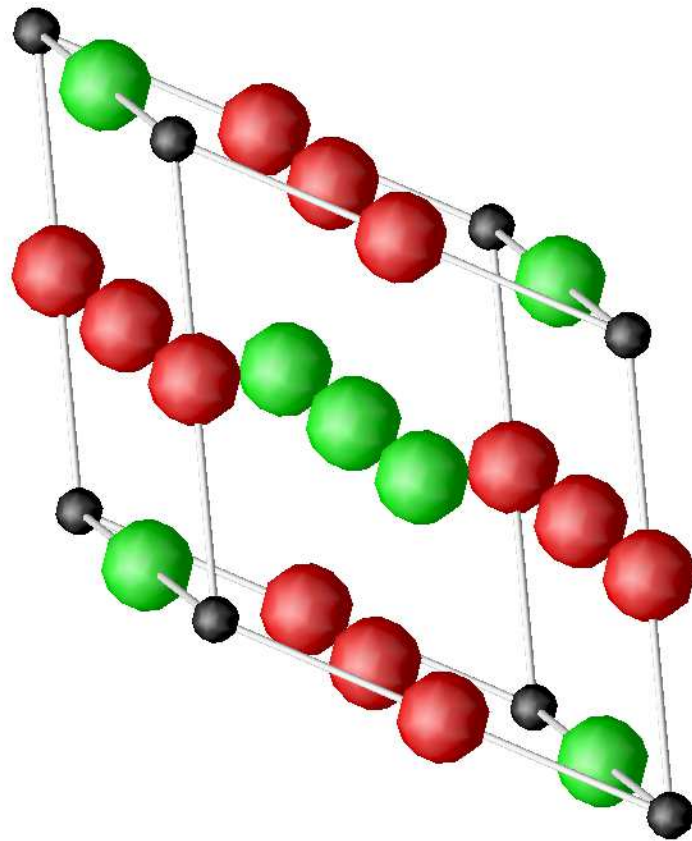


Figure 2: (Color online). Non-collinear order obtained for 8-atoms supercell with vacancy. Vacancy is shown as black spheres. Green and red spheres are Pu atoms with opposite directed total moments. The radii of spheres are proportional to the magnitude of correspondent magnetic moment.



Table 3: Magnetic properties of Pu ions calculated for 32-atoms supercell with one vacancy and IS at minimal distance. See also caption of Tab. 1.

	D, Å	$n_{atom}$	$S$	$L$	$J$	$f^6, \%$	$jj, \%$	$\mu_{eff}$	$n_f$
IS		1	0.058	0.086	0.029	98.9	98.2	0.145	6.1
Pu1	4.02	2	0.250	0.348	0.097	96.1	92.0	0.259	5.61
		2	0.195	0.267	0.073	97.1	93.8	0.225	
Pu2	2.70	1	0.009	0.015	0.006	99.8	99.7	0.064	6.22
Pu3	5.10	2	0.485	0.583	0.098	96.1	84.1	0.237	5.71
		2	0.532	0.645	0.113	95.5	82.6	0.252	
Pu4	6.91	2	0.230	0.313	0.083	96.7	92.7	0.239	5.75
		2	0.021	0.038	0.017	99.3	99.4	0.111	
Pu5	4.09	2	0.165	0.212	0.047	98.1	94.7	0.180	5.71
		2	0.122	0.155	0.033	98.7	96.1	0.153	
Pu6	2.85	2	0.057	0.081	0.024	99.1	98.2	0.132	5.78
		2	0.088	0.117	0.029	98.8	97.2	0.145	
Pu7	5.18	2	0.123	0.156	0.034	98.7	96.1	0.154	5.75
Pu8	6.91	1	0.069	0.077	0.008	99.7	97.7	0.074	5.75
Pu9	5.35	2	0.220	0.277	0.057	97.7	92.9	0.196	5.77
Pu10	6.99	2	0.343	0.448	0.105	95.8	88.9	0.261	5.78
Pu11	5.24	2	0.069	0.095	0.027	98.9	97.8	0.140	5.79
		2	0.150	0.199	0.049	98.0	95.2	0.186	

#### 4. Vacancy and Interstitial Plutonium at minimal distance

Since IS and vacancy affects on the magnetism in Pu in different ways, we can expect that their simultaneous influence could also give rise of local moment, and produce some complicated magnetic pattern.

As the first step, 32-atoms supercell with IS and vacancy at minimal distance has been investigated. Relaxation of the supercell was made with use of molecular dynamics within MEAM. Both removing one Pu atom from its site and relaxation lowers the symmetry of considered supercell and one class of Pu has been divided in 11 classes. Six of them have 2 subclasses (see Tab. 3). Small local moments also developed at Pu sites of relaxed supercell. Magnitude of moments and other results of LDA+U+SO calculation are presented in Tab. 3. Two different values of moments for one type of Pu atoms is the consequence of lowering of the symmetry of supercell due to orbital polarization. Mutual action of IS and vacancy decreases dispersion of magnitudes on different sites. The averaged value of effective moment at Pu atom is  $0.18 \mu_B$ .

Three types of Pu atoms, Pu10, Pu1, and Pu3, have the largest magnitudes of magnetic moment,  $0.261 \mu_B$ ,  $0.259 \mu_B$ , and  $0.252 \mu_B$ , correspondingly. Atoms of type Pu1 and Pu3 are the nearest to the vacancy (except IS) and have hence the largest magnetic moments in agreement with results of our previous calculation for vacancy in 8-atoms supercell (Sec. 3). Pu6 atoms belong to the first coordination sphere of vacancy but possess much smaller moment,  $\sim 0.14 \mu_B$ . This atom is positioned in the first coordination sphere of IS and, in agreement with our results for one IS in 32-atoms supercell, IS suppresses magnetism on Pu6 atom. Finally, Pu10 has a sizeable value of magnetic moment but it is smaller than that at Pu atom in the center of 32-atom supercell with single IS.

This could be explained by the action of vacancy that calls large local moments near itself and suppresses the magnetism on far standing atoms.

Simultaneous effect of IS and vacancy results in more complicated canted AFM pattern, which could not be identified with any standart type. Calculated canted AFM order is presented in Fig. 3.

### 5. Vacancy and Interstitial Plutonium at large distance

Finally, we made the same calculation for the 32-atom supercell contained IS and vacancy at the large distance. As well as in previous cases relaxation of crystal structure has been made within MEAM before band structure calculation. Considered defects also lower the symmetry and 17 new Pu classes arouse. The values of moments and contribution of coupling types and electronic configuration are presented in Tab. 4.

Like our calculation for IS and vacancy at minimal distance, local moments developed at all Pu atoms. The magnitude of moments depends on the distances to both IS and vacancy. Incommensurate magnetic order with strong noncollinearity was obtained for this type of defects position (see Fig. 4). The

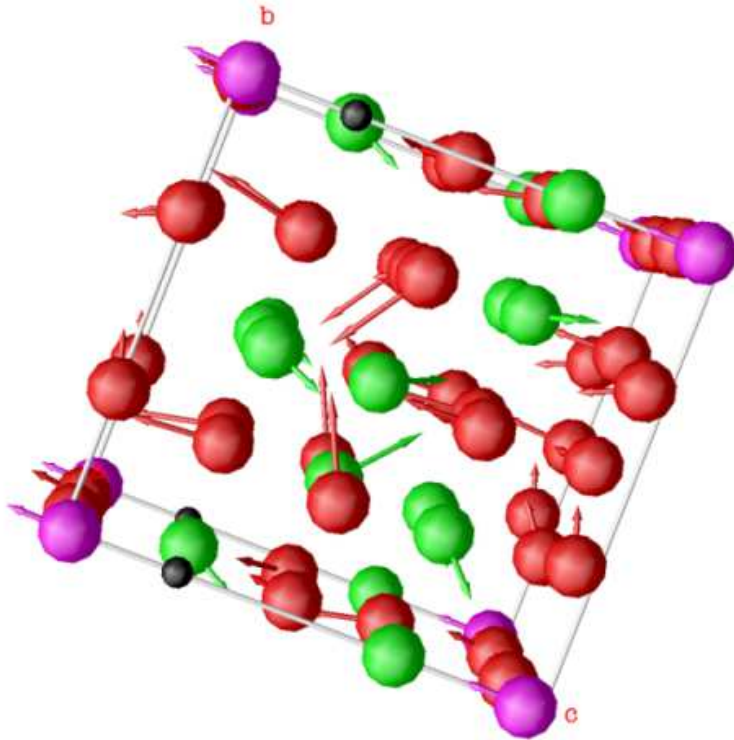


Figure 3: Ferrimagnetic order obtained for 32-atoms supercell with IS and vacancy at minimal distance. Black spheres denote vacancy, purple spheres – IS. Green and red spheres are Pu atoms with opposite signs of  $z$ -component of magnetic moment. The length of arrows is proportional to the magnitude of correspondent effective magnetic moment.

Table 4: Magnetic properties calculated for 32-atoms supercell with one vacancy and IS at large distance. See also caption of Tab. 1.

	D,Å	$n_{atoms}$	$S$	$L$	$J$	$f^6, \%$	$jj, \%$	$\mu_{eff}$	$n_f$
IS		1	.052	.083	.032	98.7	98.4	0.153	6.12
Pu1	4.26	4	.144	.176	.032	98.7	95.4	0.149	5.70
Pu2	2.79	2	.103	.141	.038	98.5	96.7	0.164	5.78
Pu3	5.01	1	.235	.333	.098	96.0	92.6	0.261	5.73
Pu4	6.67	2	.152	.188	.035	98.6	95.1	0.157	5.72
Pu5	3.77	4	.268	.361	.093	96.3	91.4	0.250	5.70
Pu6	3.11	1	.065	.091	.025	99.0	97.9	0.136	5.73
Pu7	5.25	2	.031	.039	.007	99.7	99.0	0.072	5.74
Pu8	7.12	1	.173	.219	.046	98.2	94.4	0.178	5.71
Pu9	2.63	1	.077	.128	.051	98.0	97.7	0.194	6.01
Pu10	4.90	2	.226	.276	.050	98.0	92.7	0.182	5.75
Pu11	6.83	1	.169	.276	.107	95.7	94.8	0.280	5.73
Pu12	2.79	2	.020	.031	.012	99.5	99.4	0.093	5.82
Pu13	4.87	2	.139	.181	.042	98.3	95.5	0.172	5.78
Pu14	7.29	2	.073	.131	.058	97.7	97.8	0.208	5.75
Pu15	5.23	2	.239	.303	.065	97.4	92.3	0.208	5.77
Pu16	5.42	1	.164	.228	.064	97.5	94.8	0.212	5.78
Pu17	5.02	1	.245	.312	.068	97.3	92.1	0.213	5.79

mechanism of the formation of magnetic moments was described above. The averaged magnetic moment on Pu is  $0.179 \mu_B$ .

## 6. Conclusions

Band structure calculations have been run for 4 supercells contained IS, vacancy, and both IS and vacancy at small and large distances. For the supercell with one IS ferrimagnetic order close to A-type AFM was obtained. The magnitudes of local moments are  $0.06$ – $0.46 \mu_B$  and the averaged moment is  $0.26 \mu_B$ . The largest value of magnetic moment has atoms at the largest distance from IS. Ferrimagnetic order close to C-type AFM was obtained for 8-atoms supercell with vacancy. This type of defect calls the largest moment on Pu atoms in first coordination sphere. Magnetic moments obtained in 32-atoms supercell with both IS and vacancy have smaller dispersion of magnitude  $0.1$ – $0.3 \mu_B$  and smaller averaged moment  $\sim 0.18 \mu_B$ . Simultaneous action of these defects results in incommensurate magnetic order with strong non-collinearity. Nevertheless the long range order obtained in the present work should be considered as an artifact of computation method. Our results indicate that sort range order could appear due to defects in fcc Pu. And the type of such order depends strongly on the distance to the corresponding defect. The implementation of the LDA+DMFT method is necessary to describe more accurately the magnitudes of local moment in paramagnetic phase of Pu.

Results of calculation explain presence of magnetic moment in aged Pu samples and agree well with experimental data [11, 12, 6].

Support by the Russian Foundation for Basic Research under Grant No. RFBR-07-02-00041 is gratefully acknowledged.

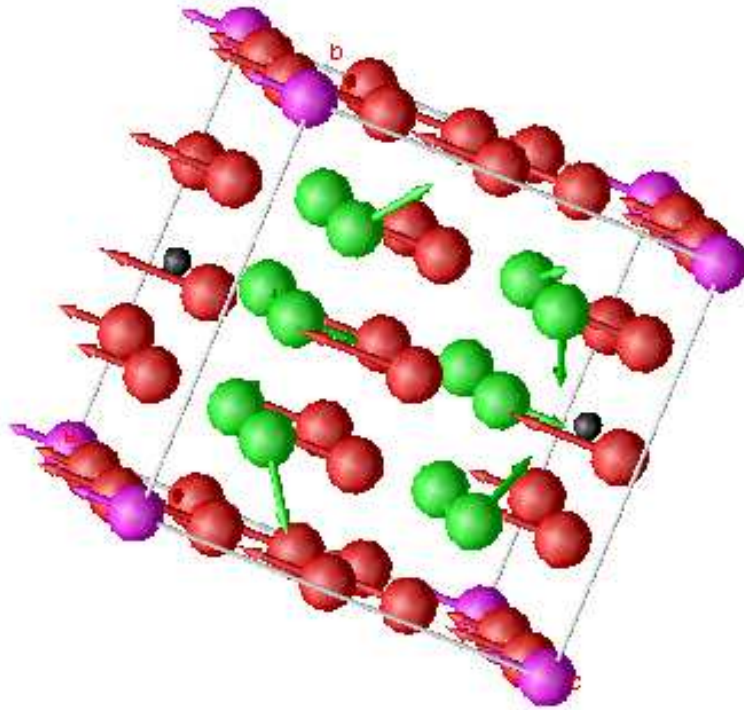


Figure 4: Ferrimagnetic order obtained for 32-atoms supercell with IS and vacancy at large distance. See also caption of Fig. 3.

- [1] S.Y. Savrasov and G. Kotliar, *Phys. Rev. Lett.* **84**, 3670 (2000).
- [2] *Plutonium – A General Survey*, edited by K.H. Lieser (Verlag, Chemie, 1974).
- [3] J. Bouchet, B. Siberchicot, F. Jollet, and A. Pasturel, *J. Phys.: Condens. Matter* **12**, 1723 (2000).
- [4] P. Söderlind, A.L. Landa, and B. Sadigh, *Phys. Rev. B* **66**, 205109 (2002).
- [5] J.C. Lashley, A. Lawson, R.J. McQueeney, and G.H. Lander, *Phys. Rev. B* **72**, 054416 (2005).
- [6] R.H. Heffner, G.D. Morris, M.J. Fluss, B. Chung, S. McCall, D.E. MacLaughlin, L. Shu, K. Ohishi, E.D. Bauer, J.L. Sarrao, W. Higemoto, and T.U. Ito, *Phys. Rev. B* **73**, 094453 (2005).
- [7] A.O. Shorikov, A.V. Lukoyanov, M.A. Korotin, and V.I. Anisimov, *Phys. Rev. B* **72**, 024458 (2005).
- [8] A.B. Shick, V.Drchal, and L. Havela, *Europhys. Lett.* **69**, 588 (2005).
- [9] P. Söderlind, *Phys. Rev. B* **77**, 085101 (2008).

- [10] R.H. Heffner, K. Ohishia, M.J. Fluss, G.D. Morrisd, D.E. MacLaughline, L. Shue, B.W. Chungc, S.K. McCallc, E.D. Bauerb, J.L. Sarraob, T.U. Itof and W. Higemotoa, *J. Alloys Comp.* **444-445** 80-83 (2007).
- [11] S.V. Verkhovkii, V.E. Arkhipov, Yu.N. Zuev, Yu.V. Piskunov, K.N. Mikhalev, A.V. Korolev, I.L. Svyatov, A.V. Pogudin, V.V. Ogloblichev, and A.L. Buzulukov, *JETP Lett.* **82**, 139 (2005).
- [12] S. Verkhovskii, Yu. Piskunov, K. Mikhalev, A. Buzlukov, A. Arkhipov, Yu. Zuev, A. Korolev, S. Lekomtsev, I. Svyatov, A. Pogudin, and V. Ogloblichev, *J. Alloys Comp.* **444-445**, 288 (2007).
- [13] M. Singh, J. Callaway, and C.S. Wang, *Phys Rev. B* **14**, 1214 (1976).
- [14] C.T. Chen, Y.U. Idzera, H.-J. Lin, N.V. Smith, G. Meigs, E. Chaban, G.H. Ho, E. Pellegrin, and F. Sette, *Phys Rev. Lett.* **75**, 152 (1995).
- [15] For the review, see *Strong Coulomb Correlations in Electronic Structure Calculations: Beyond the Local Density Approximation*, edited by V.I. Anisimov (Gordon and Breach Science Publishers, Amsterdam, 2000); V.I. Anisimov, F. Aryasetiawan, and A.I. Lichtenstein, *J. Phys.: Condens. Matter* **9**, 767 (1997).
- [16] I.V. Solovyev, A.I. Liechtenstein, and K. Terakura, *Phys. Rev. Lett.* **80**, 5758 (1998).
- [17] O.K. Andersen, *Phys. Rev. B* **12**, 3060 (1975); O. Gunnarsson, O. Jepsen, and O.K. Andersen, *ibid.* **27**, 7144 (1983).
- [18] V.I. Anisimov and O. Gunnarsson, *Phys. Rev. B* **43**, 7570 (1991).
- [19] O. Gunnarsson, O.K. Andersen, O. Jepsen, and J. Zaanen, *Phys. Rev. B* **39**, 1708 (1989).
- [20] M.I. Baskes, A.C. Lawson, S.M. Valone, *Phys. Rev. B* **72**, 014129 (2005).
- [21] S.M. Valone, M.I. Baskes, R.L. Martin, *Phys. Rev. B* **73**, 214209 (2006).
- [22] M.I. Baskes, S.Y. Hu, S.M. Valone, G.F. Wang, A.C. Lawson, *J. Computer-Aided Mater. Des.* **14**, 379-388 (2007).
- [23] V.V. Dremov, F.A. Sapozhnikov, S.I. Samarin, D.G. Modestov, N.E. Chizhkova, *J. Alloys Comp.* **444-445**, 197-201 (2007).
- [24] V.V. Dremov, A.L. Kutepov, F.A. Sapozhnikov, V.I. Anisimov, M.A. Korotin, A.O. Shorikov, D.L. Preston, M.A. Zocher, *Phys. Rev. B* **77**, 224306 (2008).
- [25] J.G. Tobin, P. Söderlind, A. Landa, K.T. Moore, A.J. Schwartz, B.W. Chung, M.A. Wall, J.M. Wills, R.G. Haire, and A.L. Kutepov, *J. Phys.: Cond. Matter* **20**, 125204 (2008); T. Björkman and O. Eriksson, *Phys. Rev. B* **78**, 245101 (2008).
- [26] V.V. Dremov, A.V. Karavaev, S.I. Samarin, F.A. Sapozhnikov, M.A. Zocher, and D.L. Preston, *J. Nucl. Mater.* **385**, 79-82 (2008).